JPET Fast Forward. Published on January 9, 2008 as DOI: 10.1124/jpet.107.128215

Design of Mutant β_2 Subunits as Decoy Molecules to Reduce the Expression of Functional Ca^{2+} Channels in Cardiac Cells

Sabine Télémaque, Swapnil Sonkusare, Terrie Grain, Sung W. Rhee, Joseph R. Stimers, Nancy J. Rusch, James D. Marsh

AFFILIATIONS: Departments of Internal Medicine (ST, TG, JDM) and Pharmacology and Toxicology (SS, SWR, JRS, NJR), College of Medicine, University of Arkansas for Medical Sciences, 4301 W. Markham # 832, Little Rock, AR 72205.

Running Title Page: **β_2 subunit mutants depress I_{Ca}**

Corresponding author:

Dr. Sabine Télémaque

Division of Cardiovascular Medicine,

Department of Internal Medicine,

College of Medicine,

University of Arkansas for Medical Sciences,

4301 W. Markham # 832, Little Rock, AR 72205.

Phone: (501) 526-7789, Fax: (501) 526-7787.

stelemaque@uams.edu

Number of text pages: 35 pages

Number of tables : 0 table

Number of figures: 8 figures

Number of references: 39 references

Number of words in Introduction: 684 words

Number of words in Abstract: 249 words

Number of words in Discussion: 1500 words

List of nonstandard abbreviations: BID, beta interaction domain; Br, brain; Ca_L, L-type Ca^{2+} channel; Ca_V, Ca^{2+} channel; $[Ca^{2+}]_{cyt}$, cytosolic Ca^{2+}; CMV, cytomegalovirus; EGTA, Ethylene glycol-bis(2-aminoethylether)-*N*,*N*,*N′*,*N′*-tetraacetic acid; GFP, green fluorescence protein; HEK,

human embryonic kidney; HEPES, (4-(2-Hydroxyethyl)piperazine-1-ethanesulfonic acid); I_{Ca}, Ca^{2+} channel current; I-V, current-voltage; Mibefradil, (1S,2S)-2-[2[[3-(2-Benzimidazolylpropyl]methylamino]ethyl]-6-fluoro-1,2,3,4-tetrahydro-1-isopropyl-2-naphthyl methoxyacetate dihydrochloride hydrate; Nifedipine, 1,4-Dihydro-2,6-dimethyl-4-(2-nitrophenyl)-3,5-pyridinedicarboxylic acid dimethyl ester ; PVDF, polyvinylidene fluoride; Triton X-100, Polyethylene glycol *tert*-octylphenyl ether; Tween-20, Polyethylene glycol sorbitan monolaurate.

Recommended section assignment: Cardiovascular

JPET Fast Forward. Published on January 9, 2008 as DOI: 10.1124/jpet.107.128215
This article has not been copyedited and formatted. The final version may differ from this version.

Abstract

Calcium influx through long-lasting ("L-type") Ca^{2+} channels (Ca_V) drives excitation-contraction in the normal heart. Dysregulation of this process contributes to Ca^{2+} overload, and interventions that reduce expression of the pore-forming α_1 subunit may alleviate cytosolic Ca^{2+} excess. As a molecular approach to disrupt the assembly of $Ca_V1.2$ (α_{1C}) channels at the cell membrane, we targeted the Ca^{2+} channel β_2 subunit, an intracellular chaperone that interacts with α_{1C} via its beta interaction domain (BID) to promote $Ca_V1.2$ channel expression. Recombinant adenovirus expressing either the full β_2 subunit (Full-β_2) or truncated β_2 subunit constructs lacking either the C-, N-terminus or both (N-BID, C-BID, BID, respectively) fused to GFP were developed as potential decoys and overexpressed in HL-1 cells. Fluorescence microscopy revealed that the localization of Full-β_2 at the surface membrane was associated with increased Ca^{2+} current mainly attributed to $Ca_V1.2$ channels. In contrast, truncated N-BID and C-BID constructs showed punctate intracellular expression, and BID showed a diffuse cytosolic distribution. Total expression of the α_{1C} protein of $Ca_V1.2$ channels was similar between groups, but HL-1 cells overexpressing C-BID and BID exhibited reduced Ca^{2+} current. C-BID and BID also attenuated Ca^{2+} current associated with another L-type Ca^{2+} channel, $Ca_V1.3$, but did not reduce transient ("T-type") Ca^{2+} currents attributed to Ca_V3 channels. These results suggest that β_2 subunit mutants lacking the N-terminus may preferentially disrupt the proper localization of L-type Ca^{2+} channels in the cell membrane. Cardiac-specific delivery of these decoy molecules *in vivo* may represent a gene-based treatment for pathologies involving Ca^{2+} overload.

Introduction

The predominant voltage-gated Ca^{2+} channels (Ca_V) in cardiac cells are the dihydropyridine-sensitive $Ca_V1.2$ (α_{1C}) channels that mediate long-lasting ("L-type") Ca^{2+} current as a critical step in excitation-contraction coupling (Bers, 2002). The $Ca_V1.2$ channels are multi-protein complexes composed of a large, pore-forming α_{1C} subunit and accessory β and α_2-δ subunits. The expression level of functional $Ca_V1.2$ channels is regulated by the β subunits (β_1, β_2, β_3, β_4), which are cytoplasmic proteins encoded by four different genes including multiple splice variants (Foell et al., 2004). The β_2 subunit is predominantly expressed in rat ventricular myocytes, although other gene families have been reported. Importantly, β_2 acts as a molecular chaperone that escorts α_{1C} to the sarcolemma to localize functional $Ca_V1.2$ channels at the surface membrane (Pragnell et al., 1994; De Waard et al., 1996; Opatowsky et al., 2003). Indeed, we recently reported that overexpression of β_2 in isolated feline ventricular myocytes significantly increases Ca^{2+} influx and cardiac contractility (Chen et al., 2005). Although mutations in the β-interaction domain (BID) of β_2 were found to abolish α_{1C}-β interaction (De Waard et al., 1994; De Waard et al., 1996), two additional protein-interaction domains (SH3 and GK) were recently identified that also may interact with α_{1C} subunit (Chen et al., 2004; Opatowsky et al., 2004; Van Petegem et al., 2004). Thus, it has been suggested that BID may not bind directly to α_{1C}, but instead is fundamentally essential for the structural integrity and bridging of the SH3 and GK domains.

Although physiologically essential to normal cardiac function, $Ca_V1.2$ channels also have been implicated in pathological processes involving Ca^{2+} overload including cardiac ischemia and myocardial stunning. In these conditions, an elevated cytosolic Ca^{2+} ($[Ca^{2+}]_{cyt}$) in the myocardial cells is associated with a loss of myofilament sensitivity to Ca^{2+} (Bolli and Marban,

1999). Moreover, Ca^{2+} overload also plays an important role in cardiac apoptosis and necrosis (Aon et al., 2003). Even under conditions in which $[Ca^{2+}]_{cyt}$ is within a normal range, it may be desirable to modestly depress $[Ca^{2+}]_{cyt}$ as a therapeutic intervention to slow atrio-ventricular conduction in atrial fibrillation or to modestly depress contractility in hypertrophic cardiomyopathy. Currently, calcium channel blockers represent the drug therapies of choice for these conditions, but several features of their properties including their short duration of action and vascular dilator effects limit their usefulness.

In this respect, a gene therapy approach designed to reduce the availability of β_2 subunits required for the expression of $Ca_V1.2$ channels may provide for the highly targeted and long-term relief of calcium overload. Accordingly, we engineered recombinant adenoviral constructs expressing truncated β_2 to provide proof of concept that mutated β_2 could potentially act as a dominant negative construct to reduce $Ca_V1.2$ channels at the surface membrane. In the present study, we expressed the recombinant adenovirus constructs in HL-1 cells, a cell line derived from AT-1 mouse atrial tumor lineage that displays many normal markers of cardiac biology. HL-1 cells spontaneously depolarize and express ion channels required for generating action potentials (White et al., 2004), and retain the signaling pathways to respond appropriately to inotropic and chronotropic agonists (Claycomb et al., 1998). The activity of the truncated β_2 constructs was compared to the effect of full length β_2, which we have shown enhances the expression of functional $Ca_V1.2$ channels in feline cardiac myocytes (Chen et al., 2005). The goal was to retain the ability of the β_2 decoys to bind to α_{1C}, but to eliminate the amino and/or carboxyl termini of β_2 that may be required for the expression of functional α_{1C} subunits in the plasma membrane, thereby "trapping" $Ca_V1.2$ channels inside the cell. We also evaluated the effect of the β_2 subunit mutants on Ca^{2+} current attributed to two other types of Ca^{2+} channels

important in pacemaker activity or contractile function. The $Ca_V1.3$ channels (α_{1D}) mediate L-type current at mid-voltages, and are approximately 10-fold less sensitive to nifedipine-induced block than $Ca_V1.2$ channels at negative membrane potentials (Koschak et al., 2001). HL-1 cells also express Ca_V3 channels that activate at much lower voltages than L-type channels, and mediate transient ("T-type") current associated with normal pacemaker activity in cardiac cells (Xia et al., 2004; Zhang et al., 2005).

JPET Fast Forward. Published on January 9, 2008 as DOI: 10.1124/jpet.107.128215
This article has not been copyedited and formatted. The final version may differ from this version.

Methods

Culture of HL-1 cells. HL-1 cells (kindly provided by Dr. W. C. Claycomb, Louisiana State University) were grown and maintained in Claycomb Medium (SAFC Biosciences, Lenexa, KS) supplemented with penicillin-streptomycin (1X) and 2 mM L-glutamine (Invitrogen, Carlsbad, CA). Following trypsinization, dissociated cells were either plated in standard 60 mm tissue culture dishes (0.8-1.0 x 10^6 cells/ml) for mRNA and/or protein expression assays or glass culture dishes (MatTek Corp, Ashland, MA) for electrophysiology (60-80 x 10^3 cells/ml). Cells were then infected for 24 to 48 hr with one of four different GFP-fused β_2 subunit constructs including full length β_2 (Full-β_2), or truncated β_2 lacking either the N-terminus (C-BID), the C-terminus (N-BID) or both termini (BID only) or with the control GFP construct. The optimal dose of crude viral stock (multiplicity of infection: 50-100) needed to optimize protein expression without visible cell death was determined by fluorescent imaging and immunoblot techniques. Experimental conditions were developed that produced >95% infection of HL-1 cells for each of the constructs studied, as previously described (Fan et al., 2003; Telemaque-Potts et al., 2003; Chen et al., 2005). All studies on HL-1 cells were performed between 24 and 48 hr post-transfection.

Detection of Ca_L channel subunit gene expression in HL-1 cells. In order to identify the endogenous β subunits expressed in HL-1 cells, total RNA was isolated from untreated HL-1 cells using a Trizol reagent (Invitrogen). First strand cDNA was synthesized using SuperScript III reverse transcriptase (Invitrogen). Primers for PCR reactions were designed to detect $Ca_V1.2$ (α_{1C}) and different β subunit isoforms (β_1, β_{2a}, $\beta_{2b,}$ β_3, β_4). Sense and antisense primers were:

α_{1C}: 5' –CCGCCCACTACCAAGATCAAC, 5' –TCGTGTCATTGACAATGCGG; covering cDNA base 2536 to 2791 (256 bp; GenBank Accession No. NM_012517.1 [rat])

JPET Fast Forward. Published on January 9, 2008 as DOI: 10.1124/jpet.107.128215
This article has not been copyedited and formatted. The final version may differ from this version.

$\beta_{1:}$ 5' –TCCAGAAGAGCGGCATGTCCC, 5' –AGGACGTACTCCCGTCTGAC; covering cDNA base 5 to 140 (136 bp; GenBank Accession No. NM_031173.2 [mouse])

β_{2a}: 5'–CGAGTACGGGTGTCCTATG, 5'–CGTCCTATCCACCAGTCAT; covering cDNA base 31 to 320 (290 bp; GenBank Accession No. NM_053851.1 [rat])

β_{2b}: 5'–AGGCAGTTGGTGTCTTCTC, 5'–CGTCCTATCCACCAGTCAT; covering cDNA base 10 to 323 (314 bp; GenBank Accession No. AF423193 [rat])

β_3: 5' –CATCCCTGGACTTCAGAAC, 5' –TGGTAGGCATCTGCATAGTC; covering cDNA base 1125 to 1301 (177 bp; GenBank Accession No. NM_007581.2 [mouse])

β_4: 5' –CTCACCATATCCCACAGCAA, 5' –TCCGGGTAATCTTCTTCCACCA covering cDNA base 1266 to 1478 (213 bp; GenBank Accession No. NM_001037099.1 [mouse]).

Reactions contained 2 μl cDNA, 10 pmol of each primer, 0.3 mM of dNTPs, 1.0 mM $MgSO_4$ and 0.5 units *Pfx* DNA polymerase (Invitrogen) mixed with 1× enhancer buffer in a total volume of 25 μl. Amplification steps included initial denaturation at 94°C for 3 min, followed by 30 cycles (denaturation for 30 s at 94°C; annealing 30 s at 53°C; extension 30 s at 68°C). A final step for product extension was performed at 68°C for 5 min. The PCR products (5 μl) were separated using a 1.2% agarose gel stained with ethidium bromide for visualization. All oligonucleotide sequences were directed toward the mouse/rat sequences of the Ca^{2+} channel subunits.

Generation of β_2 subunit constructs. A plasmid encoding the rat heart/brain β_{2a} subunit cDNA, a generous gift from Dr. E. Perez-Reyes (Perez-Reyes et al., 1992), was used as a template for generating three PCR-based mutations of the β_{2a} subunit. Briefly, cDNA encoding the N-BID fragment (bp 376-1177), BID fragment (bp 867–1177) and C-BID fragment (bp 867-2427) were amplified, digested and directionally cloned into pEGFP-C1 vector (Clontech,

Mountain View, CA), an expression vector driven by a cytomegalovirus (CMV) promoter. All β_2 subunit constructs were cloned in frame with an enhanced green fluorescence protein (GFP) reporter gene located at the amino-terminal end of the construct. A schematic representation of the various β_2 subunit adenoviral constructs is illustrated in Figure 1.

Preparation of recombinant adenovirus construct. Recombinant adenovirus constructs were prepared based on the methods described by He et al. (He et al., 1998) and made commercially available (AdEASY) by Stratagene (La Jolla, CA). The CMV-GFP-β subunit fragments were gel-purified and subcloned into the pShuttle vector, linearized and co-transformed into *E. coli* BJ5183 cells with pAdEasy-1, the adenoviral backbone. A CMV-GFP lacking any β subunit construct also was subcloned into a pShuttle vector to construct a control virus (Fan et al., 2003). Recombinants were then linearized, transfected into human embryonic kidney (HEK) 293 cells (ATCC, Manassas, VA) using the FuGene 6 reagent (Roche Molecular Systems, Alameda, CA). Virus-containing medium from HEK 293-infected cells was collected 3 to 6 days post-infection and proper expression of GFP-fused β subunits was confirmed by PCR and immunodetection. High titer viral stock was generated by several rounds of amplification in HEK 293 cells and purification by cesium chloride gradient ultracentrifugation (Niranjan et al., 1996; Telemaque-Potts et al., 2003). Final viral stock titer was determined by plaque assay (1-3 x 10^8 plaque forming unit/μl).

Immunodetection. Forty-eight hours post-infection, cells were washed twice with cold phosphate buffered saline (PBS), and then lysed in Triton lysis buffer containing 50 mM HEPES (4-(2-Hydroxyethyl)piperazine-1-ethanesulfonic acid), 150 mM NaCl, 1 mM EGTA (ethylene glycol-bis(2-aminoethylether)-*N,N,N′,N′*-tetraacetic acid), 1.5 mM $MgCl_2$, 1% Triton X-100 (polyethylene glycol *tert*-octylphenyl ether), 1% glycerol, 1 X Sigma phosphatase inhibitor

cocktail and 1X Sigma protease inhibitor cocktail. Cell lysates were incubated on ice for 15 to 20 min, centrifuged at 4°C for 15 min at 14,000*g*, and supernatants were collected. Protein concentration in supernatants was measured by the Bradford method (BioRad, Hercules, CA). Equal protein samples (40 μg total protein) were loaded on 3-8% NuPAGE tris acetate gels (Invitrogen), run and transferred to a polyvinylidene fluoride (PVDF) membrane. After blocking the membrane (Tris-buffered saline solution containing 10% non-fat dry milk and 0.1% Tween-20 (polyethylene glycol sorbitan monolaurate)), immunoblotting was performed using mouse α_{1C} monoclonal antibody (1:200; NeuroMabs, Davis, CA), mouse β-actin monoclonal antibody (1:5,000; Sigma-Aldrich, St. Louis), and mouse GFP monoclonal antibody (1:2000; Invitrogen). Corresponding secondary horseradish peroxidase-conjugated antibodies were used (1:10,000 - 1:20,000 dilutions, Jackson ImmunoResearch, West Grove, PA). Additional western blots were probed with polyclonal antibodies using methods previously published (Pesic et al., 2004). These antibodies were obtained commercially (Alomone, Jerusalem, Israel) and directed against $Ca_V1.2$ (α_{1C}), $Ca_V1.3$ (α_{1D}), $Ca_V3.1$ (α_{1G}) and $Ca_V3.2$ (α_{1H}). Protein bands were visualized by enhanced chemiluminescence, and the blots were exposed to Hyperfilm (GE Healthcare, Chicago, IL). Band densities were quantified by densitometry (GelDoc System, BioRad), analyzed with BioRad image analysis software, and normalized to β-actin expression.

Fluorescent localization of recombinant adenovirus proteins. Infected cells grown on glass bottom tissue culture dishes for 24 hr post-infection were washed, fixed in 4% paraformaldehyde and kept in the dark at 4°C until fluorescent imaging. The images were acquired using a spinning disk confocal CARV II unit (BD Biosciences, San Jose, CA) on a Zeiss 200M microscope (Thornwood, NY) fitted with a 100x/1.4 NA objective and a Retiga EXi camera (QImaging, Surrey, BC, Canada).

Whole-cell patch clamp. Functional expression of Ca^{2+} channels was evaluated using the whole-cell configuration of the patch-clamp technique (Hamill et al., 1981). After 24 hr of infection with the different β_2 constructs, culture dishes were mounted on the stage of an inverted microscope (Nikon, Japan) and HL-1 cells expressing GFP were identified by epifluorescence microscopy and selected for electrophysiological recordings. Cells were initially bathed in a solution containing 145 mM NaCl, 5.4 mM KCl, 1 mM $CaCl_2$, 1 mM $MgCl_2$, 10 mM HEPES and 5.5 mM dextrose. After formation of a conventional gigaohm seal, the patched membrane was ruptured to obtain the whole-cell configuration. Cells were then bathed in a solution that consisted of 20 mM $BaCl_2$, 115 mM N-methyl D-glucamine, 10 mM HEPES, 1 mM $MgCl_2$ and 5.5 mM dextrose (pH 7.4, 300 mOsm). The pipette solution consisted of 120 mM cesium aspartate, 30 mM cesium chloride, 0.5 mM GTP, 5 mM MgATP, 5 mM creatine phosphate and 5 mM sodium pyruvate (pH 7.2, 300 mOsm). Data acquisition and pulse generation were performed using pClamp software (Molecular Devices, Sunnyvale, CA) and an Axopatch 200A amplifier interfaced with a Digidata-1320 acquisition system (Molecular Devices). The data were sampled at 2 to 10 kHz and filtered at 1 to 5 kHz. Capacitance and series resistance compensations were used, and leak current was linearly subtracted using a P/4 protocol with a subtracting holding potential of -100 mV. Currents were normalized to cell size by dividing by cell capacitance (in pA/pF). Data analysis was performed using Clampfit (Molecular Devices) and Origin (OriginLab, Northampton, MA), as previously described (Stimers et al., 2003). Activation curves were fit by the Boltzmann equation, $I/I_{max} = A_2 + (A_1-A_2)/(1 + \exp((V-V_{1/2})/s)$; where V is the command voltage, $V_{1/2}$ is the potential of half-maximal activation, s is the slope factor, A_1 is the maximum value of the ratio I/I_{max} (fixed at 1), and A_2 is the minimum value of

the ratio I/I_{max}. Steady-state inactivation curves also were fit according to a Boltzmann function, $I/I_{max} = A_2 + (A_1-A_2)/(1 + \exp((V-V_{1/2})/s)$, to obtain half-maximal inactivation values.

Chemicals. Unless otherwise stated, all standard chemical reagents were purchased from Sigma-Aldrich (St. Louis, MO).

Statistical analysis. Data are reported as mean ± standard error of the mean. Statistical comparisons were performed using one-way ANOVA followed by *post hoc* Student-Newman-Keul's test. Values of P less than 0.05 were considered significant.

JPET Fast Forward. Published on January 9, 2008 as DOI: 10.1124/jpet.107.128215
This article has not been copyedited and formatted. The final version may differ from this version.

Results

Characterization of Ca^{2+} channel subunits in HL-1 cells. Prior to introducing β subunit decoys, we determined the native profile of β subunits in HL-1 cells. Transcripts for the $Ca_V1.2$ (α_{1C}) subunit and for multiple β subunits including β_1, β_2, β_3, and β_4 were detected (Figure 2A). Subsequently, we confirmed the presence of nifedipine-sensitive, high threshold Ca^{2+} channel current (I_{Ca}) attributed to $Ca_V1.2$ channels in these cells. Exposure of HL-1 cells to 10 μM nifedipine (n = 4) resulted in a marked inhibition of I_{Ca} elicited by stepwise 10-mV depolarizing pulses between -40 mV to +50 mV (Figure 2B). In these recordings, the I_{Ca} resistant to block by nifedipine was attributed to the presence of Ca^{2+} channel types other than $Ca_V1.2$ (Xia et al., 2003; Hansen et al., 2004; Zhang et al., 2005).

Adenovirus infection of HL-1 cells. Initial experiments assessed the potential for cytotoxicity of the adenoviral treatment. The MOI was adjusted to achieve >95% cell transduction by the adenovirus (determined by GFP fluorescence) at 48 hr after viral treatment, with minimal (<10%) cytopathic effects visible as cell detachment, rounding or blebbing. There was no evident difference in cytopathic effect between HL-1 cells treated with a control adenovirus (without construct) and the wild type or mutant constructs. To confirm that adenoviral infection with GFP-fused constructs containing β_2 subunits resulted in expression of the appropriate protein, immunoblots were performed on cell lysates collected from HL-1 cells 48 hr after adenoviral infection. The use of an antibody directed against GFP confirmed that all GFP-fused β_2 constructs were successfully expressed in the infected HL-1 cells (Figure 3, lanes 2 to 6) while no immunoreactivity was detected in untreated HL-1 cells (Figure 3, lane 1). Full β_2 was detected as a ~106 kDa protein (lane 2), whereas truncation of the amino terminus resulted in detection of C-BID at ~88 kDa (lane 3). Similarly, N-BID with a truncated carboxyl

terminus was detected at ~66 kDa (lane 4), and the isolated BID at ~42 kDa (lane 5). Control infection with GFP resulted in the expected ~30 kDa protein (lane 6). Immunoblots were also performed to assess the expression level of $Ca_V1.2$ (α_{1C}) in untreated HL-1 cells compared to HL-1 cells infected with GFP alone or GFP- fused β_2 constructs (Figure 3B). The averaged data from 6 independent blots indicated that the protein expression level of α_{1C} was similar between untreated cells (lane 1), cells infected with GFP-fused Full β_2, C-BID, N-BID or BID constructs (lanes 2 to 5), or cells infected with GFP alone (lane 6), suggesting that overexpression of the β_2 constructs did not alter the total number of $Ca_V1.2$ channels in the HL-1 cells. Similarly, overexpression of the β_2 constructs did not change the total number of $Ca_V1.3$ channels in the HL-1 cells (data not shown).

Cellular localization of various β_2 subunit adenoviral constructs. Cells were examined by fluorescence microscopy 24 hr after treatment with adenoviral vectors. Preliminary experiments demonstrated that for adenoviral infection with either the Full-β_2 construct or various mutated constructs, gene expression determined by GFP fluorescence was already present 24 hr after viral infection. Maximal *in vivo* fluorescence was observed by 48 hr; which was confirmed by immunoblots. Although the duration of gene expression was not formally investigated in this study, strong fluorescence was maintained for at least 5 days under similar experimental conditions. We postulated that overexpression of Full-β_2 subunit would promote the normal trafficking of $Ca_V1.2$ channels to the plasma membrane. However, we anticipated that truncated β_2 subunits would retain the ability to bind to the α_{1C} subunit but display abnormal protein trafficking, and thereby not localize $Ca_V1.2$ channels at the surface membrane. Compared to untreated HL-1 cells (Figure 4A), confocal images of HL-1 cells infected with GFP revealed a diffuse pattern of fluorescence in the cytosol (Figure 4B) as reported previously in

isolated cardiomyocytes (Telemaque-Potts et al., 2003; Chen et al., 2005). In contrast, overexpression of Full-β_2 produced sarcolemmal localization (Figure 4C, arrows), whereas C-BID and N-BID fusion proteins appeared primarily localized to intracellular vesicles (Figures 4D and 4E, respectively). Overexpression of BID produced a diffuse reticular pattern suggestive of cytosolic localization (Figure 4F). Thus, the truncated β_2 subunits showed punctate or diffuse intracellular localization that was distinctly different from the sarcolemmal localization of full-length β_2. We also attempted to localize endogenous α_{1C} subunit by immunostaining, using two different commercially available antibodies against $Ca_V1.2$ channels but were unable to detect a specific signal at the cell membrane (Supplemental Figure A and Supplemental Figure B).

Effect of overexpression of β_2 adenoviral constructs on I_{Ca}. Subsequently, we compared the impact of overexpressing the β_2 adenoviral constructs (24 hr post infection) on whole-cell Ca^{2+} channel current (I_{Ca}) elicited by 10-mV depolarizing steps from a holding potential of -40 mV to potentials between -40 mV and +50 mV (Figure 5A). Initial studies suggested that this pulse protocol primarily activated high-threshold, nifedipine-sensitive $Ca_V1.2$ channels (Figure 2B). Compared to cells infected with GFP alone (Figure 5A), overexpression of Full-β_2 markedly increased the membrane density of I_{Ca} (Figure 5B) as reflected in the enhanced amplitude of the current-voltage (I-V) curve (Figure 5F). Current densities were ~2.5-fold higher at the peak of the I-V curve in Full-β_2 overexpressing cells compared to the cells overexpressing GFP alone (-17.9 ± 3.0 pA/pF and -7.2 ± 0.6 pA/pF, respectively; n = 10-12). To test the hypothesis that truncated β_2 subunits serve as dominant negative mutants, cells were infected with adenoviral constructs expressing N-BID, C-BID or BID. Recordings of whole-cell I_{Ca} in these cells are depicted in Figure 5 (C to E, respectively), and average I-V curves are plotted in Figure 5F (n = 7-10). Cells infected with N-BID (Figure 5C) showed I_{Ca} densities similar to GFP-infected cells

(Figure 5A), as verified by similar I-V curves. However, I_{Ca} was markedly reduced in C-BID and BID-overexpressing cells (Figure 5D and E, respectively) as compared to GFP alone (Figure 5A). Overexpression of truncated C-BID and BID significantly decreased I_{Ca} density at the peak of the I-V curve to -2.7 ± 0.33 pA/pF and -2.5 ± 0.7 pA/pF, respectively, compared to -7.2 ± 0.6 pA/pF in cells infected with GFP alone. Although Ca^{2+} channel β subunits can influence Ca^{2+} current kinetics (Dolphin, 2003), we did not observe consistent changes in the average inactivation rate constant (599 ± 50 msec) determined for the peak Ca^{2+} current elicited at +20 mV between HL-1 cells overexpressing the GFP, C-BID and BID constructs.

Effect of overexpression of C-BID and BID on voltage-dependent activation and inactivation of I_{Ca}. Although we hypothesized that C-BID and BID reduced I_{Ca} in HL-1 cells by retaining $Ca_V1.2$ channels intracellularly, we investigated the possibility that voltage-dependent gating also was altered. The voltage-dependence of activation was evaluated by holding cells at -55 mV and imposing 10-mV depolarizing steps between -50 mV and +20 mV. Peak current at each voltage was plotted as a ratio of maximal current elicited at +20 mV, and the data were fit by a Boltzmann equation to obtain half-activation voltages ($V_{1/2}$). The resulting activation curves in Figure 6A revealed no significant difference (n= 4-5) in $V_{1/2}$ values between cells overexpressing GFP (-14 ± 1 mV), C-BID (-12 ± 1 mV), or BID (-13 ± 1 mV). Inactivation was assessed by subjecting cells to 1400-ms prepulse voltages (10-mV steps) between -50 mV and 30 mV from a holding potential of -55 mV. Cells were briefly returned to -55 mV for 20 msec, and then pulsed to +20 mV to assess the effect of inactivating prepulses on channel availability. Peak current at each pre-pulse voltage was plotted as the ratio of maximal current elicited from a holding potential of -55 mV. Figure 6B shows data fit with the Boltzmann function, and reveals that half-inactivation voltages ($V_{1/2}$) were not significantly different (n = 4-

JPET Fast Forward. Published on January 9, 2008 as DOI: 10.1124/jpet.107.128215
This article has not been copyedited and formatted. The final version may differ from this version.

5) between HL-1 cells overexpressing GFP (-7 ± 2 mV), C-BID (-3 ± 2 mV) and BID (-5 ± 1 mV).

Effect of overexpression of C-BID and BID on Ca^{2+} channels other than $Ca_V1.2$. The finding that C-BID and BID suppressed functional $Ca_V1.2$ channels raised the important question of whether this dominant negative effect was $Ca_V1.2$ -specific, or if it extended to other types of Ca^{2+} channels. Particularly, L-type Ca^{2+} currents contributed by $Ca_V1.3$ channels (α_{1D}) have been reported in HL-1 cells (Xia et al., 2004). The $Ca_V1.3$ channels can be distinguished from high threshold $Ca_V1.2$ channels by their activation at mid-voltages and lower sensitivity to nifedipine at negative membrane potentials (Xia et al., 2004; Zhang et al., 2005; Xu and Lipscombe, 2001; Koschak et al., 2001; Zhang et al., 2005; Striessnig et al., 2006). Low-threshold, transient ("T-type") Ca^{2+} currents ascribed to Ca_V3 ($\alpha_{1G,}$ α_{1H}) channels also have been described in HL-1 atrial cells (Xia et al., 2003; Hansen et al., 2004; Yang et al., 2005). To collectively activate L-type and T-type channels to obtain "total current", we imposed progressive 10-mV depolarizing steps over a wide voltage range from -80 mV to +50 mV. Total current was suppressed in HL-1 cells overexpressing C-BID and BID compared to those expressing only the GFP construct (Figure 7A). Subsequently, the addition of 10 μM nifedipine revealed two components of total I_{Ca}. The nifedipine-resistant, residual I_{Ca} showed peak activation at +10 mV, revealing lower threshold Ca^{2+} current (Figure 7B). Digital subtraction of this I_{Ca} component from total current revealed the nifedipine-sensitive I_{Ca} attributed to $Ca_V1.2$ channels that maximally activated at +30 mV (Figure 7C). Notably, the I-V curve for the low threshold, nifedipine-resistant I_{Ca} was significantly suppressed by C-BID and BID (Figure 7B), suggesting that the dominant negative effect of these β_2 subunit mutants extends to Ca^{2+} channels other than $Ca_V1.2$.

Based on these findings, we questioned whether C-BID and BID act nonspecifically to suppress both T-type and L-type Ca^{2+} currents. Notably, the surface localization of L-type channels, including $Ca_V1.2$ and $Ca_V1.3$, is thought to rely at least partly on β subunits (Catterall et al., 2005). In contrast, T-type channels are missing the known motifs required for β subunit interaction (Perez-Reyes, 1998; Perez-Reyes, 2003; Catterall et al., 2005). To confirm the expression of both $Ca_V1.3$ and Ca_V3 channels in the HL-1 cells, and thus a possible contribution to nifedipine-resistant I_{Ca}, we probed western blots with α_1-subtype specific antibodies using mouse brain (Br) as a positive control in each of the left lanes (Figure 8A). In addition to detecting $Ca_V1.2$, α_1 subunits corresponding to $Ca_V1.3$, $Ca_V3.1$ and $Ca_V3.2$ were evident. Subsequently, we applied a depolarizing pulse between -80 mV and -10 mV to cells overexpressing GFP, C-BID or BID to maximally activate low threshold, T-type (Ca_V3) channels, but avoid activation of mid ($Ca_V1.3$) and high ($Ca_V1.2$) threshold L-type channels (Figure 8B, upper traces). To further isolate T-type current, mibefradil (7 μM), a preferential blocker of T-type channels (Martin et al., 2000; Xia et al., 2003) was applied and peak mibefradil-sensitive current elicited at -10 mV was calculated by digital subtraction (Figure 8B, lower traces). This transient current was fully intact after BID and C-BID overexpression, suggesting that the decoy effect of the β_2 subunit mutants does not extend to T-type channels (Figure 8). Rather, the dominant negative effect of C-BID and BID on nifedipine-resistant current apparently reflects an action on $Ca_V1.3$ channels or other Ca^{2+} channel types.

Discussion

The results of this study provide initial evidence that gene transfer of truncated β_2 subunits into HL-1 cells prevents the proper localization of $Ca_V1.2$ channels in the surface membrane. We took advantage of the chaperone function of the β_2 subunit to alter functional Ca_L channel expression using overexpressed truncated β_2 subunit mutants in HL-1 cells. These mutants were designed to bind the pore-forming α_{1C} subunits but prevent their proper insertion at the surface membrane to form functional Ca_L channels. We have demonstrated that two engineered β_2 subunit mutants, C-BID and BID, can serve a dominant negative function in HL-1 cells, disrupt sarcolemmal localization of $Ca_V1.2$ channels, and specifically decrease I_{Ca}. Thus, the findings establish the principle that engineered β_2 subunits represent a viable molecular approach for reducing the number of functional $Ca_V1.2$ channels in cardiomyocytes. In our experiments, the adenoviral delivery system appears to be highly effective in delivering the β_2 subunit constructs to the HL-1 cells, and the cognate proteins were readily detected. We previously used adenoviral delivery to introduce the full-length β_2 subunit into isolated feline ventricular myocytes to confirm the important role of this regulatory subunit in promoting $Ca_V1.2$ channel expression (Chen et al., 2005). In this earlier study performed in adult feline cardiomyocytes, we established that adenoviral-mediated gene delivery can indeed alter $Ca_V1.2$ channel expression and function within 24 to 48 hr, a time course similar to that for HL-1 cells.

In the present study, we also examined the dominant negative effects of C-BID and BID on additional Ca^{2+} channels co-expressed in HL-1 cells with $Ca_V1.2$. In our cells, mibefradil-sensitive, T-type current was not attenuated by either β_2 subunit mutant, consistent with reports that Ca_V3 channels do not have binding motifs to permit β subunit interaction (Perez-Reyes, 1998; Perez-Reyes, 2003; Catterall et al., 2005). However, other components of nifedipine-

resistant current were suppressed by gene delivery of C-BID and BID. One target probably was the $Ca_V1.3$ channel that provides L-type current at mid-voltages in HL-1 cells, and is 10-fold less sensitive to nifedipine than $Ca_V1.2$ channels. Although precise identification of $Ca_V1.3$ current is difficult due to the lack of a specific antagonist, members of the Ca_V1 gene family including $Ca_V1.3$ share an α- interactive domain (AID) that enables α_1 - β interaction (Catterall et al., 2005). Thus, a shared feature of the Ca_V1 gene family may be susceptibility to dominant negative β_2 mutants. In this regard, one potential therapeutic benefit of our mutants may include the treatment of supraventricular tachyarrhythmias, since atrial cells appear to densely express $Ca_V1.3$ channels which contribute to normal rhythmicity (Zhang et al., 2005). In contrast, $Ca_V1.3$ channels are only sparsely expressed in ventricular tissues and $Ca_V1.2$ channels appear to be the primary pathway for voltage-gated Ca^{2+} influx. Thus, disruption of expression of $Ca_V1.2$ channels by our β_2 subunit mutants may be beneficial in pathologies involving Ca^{2+} overload as a strategy to depress $[Ca^{2+}]_{cyt}$ and restore normal contractility.

Our findings also provide initial insight into the interactions between the α_{1C} subunit and truncated β_2 subunit decoys that may be required to interrupt the trafficking of functional Ca_L channels to the surface membrane. In contrast to the observation that overexpression of the full length β_2 subunit at the surface membrane was associated with increased I_{Ca}, the highly distinctive vesicular patterns for N-BID and C-BID localization and the reticular pattern for BID suggest disruption of proper localization of Ca_L channel subunits. Indeed, each of the truncated β_2 subunit was designed to retain the central BID sequence necessary for α_{1C} - β interaction, but at least one of the two additional protein-interaction domains (SH3 and GK) recently reported to be required for channel assembly was eliminated (Chen et al., 2004; Opatowsky et al., 2004; Van Petegem et al., 2004). Thus, the SH3 domain was absent in C-BID, a significant portion of the

GK domain was missing in N-BID whereas the SH3 domain and a significant portion of the GK domain were missing in BID. In each case, the localization of β_2 subunits was abnormal, supporting earlier reports that the β subunits rely on at least three domains in the molecule to confer structural integrity.

Although all three truncated β_2 subunits resulted in altered cellular localization, only C-BID and BID acted as dominant negative subunits by markedly depressing I_{Ca} in the HL-1 cells. It seems logical to assume that the overexpression of the two successful β_2 mutants, C-BID and BID, overwhelmed interactions between the endogenous α_{1C} and β subunits to sequester α_{1C} subunit. However, the abnormal vesicular localization of N-BID did not confer a decoy function, suggesting that it did not successfully compete for the α_{1C} subunit although it shared the BID binding site with the C-BID and BID negative constructs. This lack of dominant-negative effect of N-BID is consistent with previous observations that a short N-terminus isoform of β_1 subunit can modulate the gating of cardiac $Ca_V1.2$ channels, without promoting membrane trafficking of the channel complex (Cohen et al., 2005). Interestingly, a recent report demonstrated a link between the $Ca_V1.2$ activity and the cell endocytic machinery. In that study, the authors observed a reduction in the number of channels present at the plasma membrane, when the SH3 domain of the β subunit (also located in the N-terminus) was expressed in oocytes (Gonzalez-Gutierrez et al., 2007). The removal of the channels from the membrane by this β_2-SH3 construct is not consistent with our observation that N-BID had no effect on Ca^{2+} currents. This suggests that additional portions of the N-terminus of the β subunit may be involved in the regulation of the turnover of the L-type Ca^{2+} channels. Alternatively, it is possible that the spatial cellular localization of N-BID in these vesicle-like compartments may prevent binding interaction with the endogenous α_{1C} protein.

Our study has several limitations. First, the HL-1 cells represent an atrial cell line that expresses robust Ca^{2+} currents and other markers of cardiac function, suggesting that it is a useful model in which to study Ca^{2+} channel regulation (Claycomb et al., 1998; White et al., 2004; Xia et al., 2004). However, the effectiveness of our dominant negative β_2 constructs clearly may differ between HL-1 cells and native cardiac cells that may express different levels of endogenous β subunits or even process the mutant β subunits differently**.** Indeed, the success of our β_2 subunit mutants to reduce Ca^{2+} current in cardiac myocytes will depend on the rate of L-type channel turnover in the surface membrane *in vivo*. The precise turnover rate is unknown, but the fact that changes in Ca^{2+} current in response to norepinephrine or thyroid hormone are evident within 24 to 48 hr suggests that the membrane turnover of L-type Ca^{2+} channels is a highly dynamic process (Maki et al., 1996; Kim et al., 1987)**.** Second, we did not attempt to pinpoint the cellular sites involved in the aberrant localization of the C-BID, N-BID and BID mutants. Further detailed co-localization studies will be needed to identify the cellular compartments or organelles that account for these expression patterns.

Although our initial attempt to detect by immunostaining the endogenous α_{1C} subunit in the HL-1 cells was not successful (Supplemental Figure A and Supplemental Figure B), we believe that co-localization of the endogenous α_{1C} subunit with the GFP-tagged β_2 subunit constructs would provide important insights into the mechanism by which these β_2 subunits affect Ca^{2+} channel function. Finally, structure-function studies are needed to optimize the design of dominant negative β_2 constructs to obtain high affinity molecules that serve as effective decoys for the L-type Ca^{2+} channels as a prelude to expressing it specifically in heart.

Importantly, new molecular approaches designed to down-regulate L-type Ca^{2+} channel subunits in cardiac myocytes represent alternatives to the traditional use of organic Ca^{2+} channel

blocking drugs to attenuate $[Ca^{2+}]_{cyt}$. The concept of directly titrating the number of Ca^{2+} channel proteins rather than altering the open-state probability of an existing Ca^{2+} channel population may have advantages, particularly if coupled to a cardiac-specific delivery system to provide durability of effect. For example, work by others shows that *in vitro* gene knockdown of the β_2 subunit using RNA interference technology significantly decreased calcium transients in neonatal rat cardiomyocytes, prevented an increase in relative cell size, and abrogated phenylephrine-induced protein synthesis in a cellular model of hypertrophy (Cingolani et al., 2007). Furthermore, in an aortic-banded rat model of left ventricular hypertrophy, the same authors showed that knockdown of the β_2 subunit was capable of attenuating cardiac hypertrophy without compromising systolic performance, suggesting that the targeted suppression of pathologies involving Ca^{2+} overload may be possible (Cingolani et al., 2007). The adenoviral vectors used in our study are primarily useful *in vitro* for proof-of-concept, as they are not regarded as ideal clinical vectors due to their immunogenic nature. However, other vectors including adeno-associated viruses containing cardiac-specific promoters may permit targeted knockdown of L-type channels in the heart.

In summary, the data presented in the current study do support the concept that adenovirus-mediated gene transfer of dominant negative β_2 subunit mutants can effectively and specifically modulate L-type calcium channel expression and function in the HL-1 cell model system of cardiomyocytes.

Acknowledgments

The authors would like to thank Drs Zhen Wang and Larisa Buzdugan for their excellent technical support and GibAnn Berryhill for her assistance in preparing the manuscript.

The mouse α_{1C} subunit monoclonal antibody (clone L57/46) used in the present study was developed by and/or obtained from the UC Davis/NINDS/NIMH NeuroMab Facility and maintained by the Department of Pharmacology, School of Medicine, University of California, Davis, CA 95616.

References

Aon MA, Cortassa S, Marban E and O'Rourke B (2003) Synchronized whole cell oscillations in mitochondrial metabolism triggered by a local release of reactive oxygen species in cardiac myocytes. *J Biol Chem* **278**:44735-44744.

Bers DM (2002) Cardiac excitation-contraction coupling. *Nature* **415**:198-205.

Bolli R and Marban E (1999) Molecular and cellular mechanisms of myocardial stunning. *Physiol Rev* **79**:609-634.

Catterall WA, Perez-Reyes E, Snutch TP and Striessnig J (2005) International Union of Pharmacology. XLVIII. Nomenclature and Structure-Function Relationships of Voltage-Gated Calcium Channels. *Pharmacol Rev* **57**:411-425.

Chen X, Zhang X, Kubo H, Harris DM, Mills GD, Moyer J, Berretta R, Potts ST, Marsh JD and ouser SR (2005) Ca2+ Influx-induced sarcoplasmic reticulum Ca2+ overload causes mitochondrial-dependent apoptosis in ventricular myocytes. *Circ Res* **97**:1009-1017.

Chen Y-H, Li M-H, Zhang Y, He L-L, Yamada Y, Fitzmaurice A, Shen Y, Zhang H, Tong L and Yang J (2004) Structural basis of the subunit interaction of voltage-gated Ca^{2+} channels. *Nature* **429**:675-680.

Cingolani E, Ramirez Correa GA, Kizana E, Murata M, Cho HC and Marban E (2007) Gene Therapy to Inhibit the Calcium Channel {beta} Subunit: Physiological Consequences and Pathophysiological Effects in Models of Cardiac Hypertrophy. *Circ Res* **101**:166-175.

Claycomb WC, Lanson NA, Stallworth BS, Egeland DB, Delcarpio JB, Bahinski A and Izzo N (1998) HL-1 cells: a cardiac muscle cell line that contracts and retains phenotypic characteristics of the adult cardiomyocyte. *Proc Natl Acad Sci USA* **95**:2979-2984.

Cohen RM, Foell JD, Balijepalli RC, Shah V, Hell JW and Kamp TJ (2005) Unique modulation of L-type Ca2+ channels by short auxiliary {beta}1d subunit present in cardiac muscle. *AJP - Heart and Circulatory Physiology* **288**:H2363-H2374.

De Waard M, Pragnell M and Campbell KP (1994) Ca2+ channel regulation by a conserved beta subunit domain. *Neuron* **13**:495-503.

De Waard M, Scott VE, Pragnell M and Campbell KP (1996) Identification of critical amino acids involved in α1–β interaction in voltage-dependent Ca^{2+} channels. *FEBS Letters* **380**:272-276.

Fan QI, Vanderpool KM, O'Connor J and Marsh JD (2003) Decoy calcium channel β subunits modulate contractile function in myocytes. *Mol Cell Biochem* **242**:3-10.

Foell J, Balijepalli R, Delisle B, Yunker A, Robia S, Walker JW, McEnery M, January C and Kamp T (2004) Molecular heterogeneity of calcium channel B-subunits in canine and human heart: evidence for differential subcellular localization. *Physiol Genomics* **17**:183-200.

Gonzalez-Gutierrez G, Miranda-Laferte E, Neely A and Hidalgo P (2007) The Src Homology 3 Domain of the β–subunit of voltage-gated calcium channels promotes endocytosis via dynamin interaction. *J Biol Chem* **282**:2156-2162.

Hamill O, Marty A, Neher E, Sakmann B and Sigworth F (1981) Improved patch-clamp techniques for high resolution current recording from cells and cell free membrane patches. *Pflugers Arch* **391**:85-100.

Hansen JP, Chen RS, Larsen JK, Chu PJ, Janes DM, Weis KE and Best PM (2004) Calcium channel [gamma]6 subunits are unique modulators of low voltage-activated (Cav3.1) calcium current. *J Mol Cell Cardiol* **37**:1147-1158.

He TC, Zhou S, da Costa LT, Yu J, Kinzler KW and Vogelstein B (1998) A simplified system for generating recombinant adenoviruses. *Proc Natl Acad Sci USA* **95**:2509-14.

Kim D, Marsh JD and Smith TW (1987) Effects of thyroid hormone on slow Ca channel function in cultured chick ventricular cells. *J Clin Invest* **80**:88-94.

Koschak A, Reimer D, Huber I, Grabner M, Glossmann H, Engel J and Striessnig J (2001) alpha 1D (Cav1.3) Subunits Can Form L-type Ca2+ Channels Activating at Negative Voltages. *J Biol Chem* **276**:22100-22106.

Maki TM, Gruver EJ, Davidoff AJ, Izzo N, Toupin D, Colucci W, Marks AR and Marsh JD (1996) Regulation of calcium channel expression in neonatal myocytes by catecholamines. *J Clin Invest* **97**:656-663.

Martin RL, Lee JH, Cribbs LL, Perez-Reyes E and Hanck DA (2000) Mibefradil Block of Cloned T-Type Calcium Channels. *J Pharmacol Exp Ther* **295**:302-308.

Niranjan V, Telemaque S, deWit D, Gerard RD and Yanagisawa M (1996) Systemic hypertension induced by hepatic overexpression of human preproendothelin-1 in rats. *J Clin Invest* **98**:2364-2372.

Opatowsky Y, Chen CC, Campbell KP and Hirsch JA (2004) Structural analysis of the voltage-dependent calcium channel β subunit functional core and its complex with the α_1 interaction domain. *Neuron* **42**:387-399.

Opatowsky Y, Chomsky-Hecht O, Kang MG, Campbell KP and Hirsch JA (2003) The voltage-dependent calcium channel β subunit contains two stable interacting domains. *J Biol Chem* **278**:52323-52332.

Perez-Reyes E, Castellano A, Kim HS, Bertrand P, Baggstrom E, Lacerda AE, Wei X and Birnbaumer L (1992) Cloning and expression of a cardiac/brain β subunit of the L-type calcium channel. *J Biol Chem* **267**:1792-1797.

Perez-Reyes E (1998) Molecular Characterization of a Novel Family of Low Voltage-Activated, T-Type, Calcium Channels. *Journal of Bioenergetics and Biomembranes* **30**:313-318.

Perez-Reyes E (2003) Molecular Physiology of Low-Voltage-Activated T-type Calcium Channels. *Physiol Rev* **83**:117-161.

Pesic A, Madden JA, Pesic M and Rusch NJ (2004) High blood pressure upregulates arterial L-type Ca2+ channels: is membrane depolarization the signal? *Circ Res* **94**:e97-e104.

Pragnell M, DeWaard M, Mori Y, Tanabe T, Snutch TP and Campbell KP (1994) Calcium channel β-subunit binds to a conserved motif in the I-II cytoplasmic linker of the α_1-subunit. *Nature* **368**:67-70.

Stimers JR, Ha J and Rock T.M. (2003) Electrical remodeling caused by hypertrophy in HL-1 cells. *Circulation* **108**:IV56 (Abstract).

Striessnig J, Koschak A, Sinnegger-Brauns MJ, Hetzenauer A, Nguyen NK, Busquet P, Pelster G and Singewald N (2006) Role of voltage-gated L-type Ca2+ channel isoforms for brain function. *Biochem Soc Trans* **34**:903-909.

Telemaque-Potts S, John SK, Grain T, Potts JT and Marsh JD (2003) Expression of β2 subunit mutants alters localization of L-type calcium channels in rat adult cardiomyocytes. *FASEB J* **17(4, Part I)**:A537 (Abstract).

Van Petegem F, Clark KA, Chatelain FC and Minor DL (2004) Structure of a complex between a voltage-gated calcium channel β-subunit and an α-subunit domain. *Nature* **429**:671-675.

White SM, Claycomb W and Constantin PE (2004) Cardiac physiology at the cellular level: use of cultured HL-1 cardiomyocytes for studies of cardiac muscle cell structure and function. *Am J Physiol Heart Circ Physiol* **286**:H823-829.

Xia M, Salata JJ, Figueroa DJ, Lawlor A-M, Liang HA, Liu Y and Connolly TM (2004) Functional expression of L- and T-type Ca2+ channels in murine HL-1 cells. *J Mol Cell Cardiol* **36**:111-119.

Xia M, Imredy JP, Santarelli VP, Liang HA, Condra CL, Bennett P, Koblan KS and Connolly TM (2003) Generation and Characterization of a Cell Line with Inducible Expression of Cav3.2 (T-Type) Channels. *ASSAY and Drug Development Technologies* **1**:637-645.

Xu W and Lipscombe D (2001) Neuronal CaV1.3{alpha}1 L-Type Channels Activate at Relatively Hyperpolarized Membrane Potentials and Are Incompletely Inhibited by Dihydropyridines. *Journal of Neuroscience* **21**:5944-5951.

Yang Z, Shen W, Rottman JN, Wikswo JP and Murray KT (2005) Rapid stimulation causes electrical remodeling in cultured atrial myocytes. *J Mol Cell Cardiol* **38**:299-308.

Zhang Z, He Y, Tuteja D, Xu D, Timofeyev V, Zhang Q, Glatter KA, Xu Y, Shin HS, Low R and Chiamvimonvat N (2005) Functional Roles of Cav1.3({alpha}1D) Calcium Channels in Atria: Insights Gained From Gene-Targeted Null Mutant Mice. *Circulation* **112**:1936-1944.

Footnotes

This work was supported in part by the UAMS Department of Internal Medicine Departmental Research Endowments (to ST and to JDM), UAMS Department of Pharmacology and Toxicology Research Funds (to JRS), the Department of Veterans Affairs in the form of a VA Merit Award to JDM, and USPHS R01 HL-68406 and R01 HL-050818 (to NJR) from the National Institutes of Health. The UC Davis/NINDS/NIMH NeuroMab Facility (mouse α_{1C} subunit antibody) is supported by NIH grant U24NS050606.

A preliminary version of some of these results has been presented in abstract form [Sonkusare S, Stimers JR, Grain T, Marsh JD, and Télémaque S (2006) Expression of β_2 subunit mutants alters calcium currents in HL-1 cells. *FASEB J.* **20**(5, Part II): A1114].

ST and SS contributed equally to this work.

Address reprint requests to: Dr. Sabine Télémaque, Division of Cardiovascular Medicine, Department of Internal Medicine, College of Medicine, University of Arkansas for Medical Sciences, 4301 W. Markham # 832, Little Rock, AR 72205. E-mail: stelemaque@uams.edu

Legends for Figures

Figure 1. Schematic representation of rat cDNA constructs expressing the full-length β_2 subunit (Full-β_2) and truncated β_2 subunits (N-BID, BID and C-BID).

Figure 2. **A,** agarose gel of PCR products corresponding to the α_{1C} subunit of $Ca_V1.2$, and native β_1, β_{2a}, β_{2b}, β_3 and β_4 subunits in HL-1 cells. **B**, representative whole-cell Ca^{2+} channel current (I_{Ca}) recorded from an HL-1 cells before (left) and after (right) exposure to 10 μM nifedipine for 2 min. Similar results were obtained in 3 other nifedipine-treated cells.

Figure 3. Immunoblot of total cell lysates from HL-1 cells (40 μg protein/lane) infected with five different adenoviruses expressing GFP alone or GFP-fused β_2 subunit constructs. Untreated cells (lane 1); cells infected with Full-β_2 (~ 106 kDa, lane 2); C-BID (~ 88 kDa, lane 3), N-BID (~ 66 kDa, lane 4); BID (~ 42 kDa, lane 5) and GFP (~ 30 kDa, lane 6). **A,** immunodetection using GFP antibody. **B,** gel blots depicting expression of α_{1C} (240 and ~ 200 kDa bands) and β-actin (~ 42 kDa, internal loading control) using specific antibodies. Data are shown as mean ± SEM of 6 independent experiments.

Figure 4. Fluorescence microscopic images of HL-1 cells show a different localization pattern for each β_2 subunit construct at 24 hr post-infection. Untreated cells (**A**); cells infected with GFP (**B**), Full-β_2 (**C**); C-BID (**D**), N-BID (**E**); BID (**F**). Arrows indicate the cell membrane localization of fluorescence. Calibration bar = 10 μm.

Figure 5. Effect of adenovirus-mediated overexpression of Full-β_2 subunit and different truncated β_2-subunit constructs on I_{Ca} primarily attributed to $Ca_V1.2$ channels in HL-1 cells. **A,**

representative raw current traces (-30 mV to +20 mV) of whole-cell I_{Ca} measured in cells expressing GFP (**A**), Full-β_2 (**B**), N-BID (**C**), C-BID (**D**) or BID (**E**). Average current-voltage (I-V) data were normalized to cell capacitance. Cells were held at -40 mV and given a series of 200 ms pulses from -40 mV to +50 mV, using progressive 10 mV depolarizing steps. **F**, The I-V relationship shows I_{Ca} as a function of membrane potential at which it was elicited in cells expressing GFP (■), Full-β_2 (Δ), N-BID (○), C-BID (□) or BID (●). Average peak I_{Ca} was plotted versus voltage. Data are shown as mean ± SEM. §: $P< 0.05$ between Full-β_2-infected cells and cells infected with GFP alone (n = 10-12). *: $P< 0.05$ between BID-infected cells and cells infected with GFP alone (n = 10 each). #: $P< 0.05$ between C-BID-infected cells and cells infected with GFP alone (n = 7-10).

Figure 6. Effect of adenovirus-mediated overexpression of different truncated β_2 subunit constructs on voltage-dependent activation and inactivation of Ca^{2+} channels primarily attributed to $Ca_V1.2$. **A,** Activation curve showing normalized currents elicited at various command potentials (-50 to +20 mV) from a holding potential of -55 mV. I/I_{max} value was calculated at each voltage and plotted against the voltage. The solid lines represent fits with the Boltzmann function. There was no significant difference in $V_{1/2}$ between cells overexpressing GFP compared to C-BID and BID (n = 4-5). **B,** Voltage-dependent inactivation of Ca^{2+} channel currents using a double-pulse protocol. Pre-pulse voltage steps (-50 mV to 30 mV) from a holding potential of -55 mV were imposed, and channel availability evaluated by a subsequent voltage pulse from -55 mV to +20 mV. I/I_{max} value was calculated at each voltage and plotted against the voltage. Data fit with the Boltzmann function revealed similar half-inactivation

voltages for GFP, C-BID and BID overexpressing cells. Data values are expressed as mean ± SEM (n= 4-5).

Figure 7. Calcium current separation using nifedipine to determine the effect of C-BID and BID overexpression on different Ca^{2+} current components in HL-1 cells. Currents were elicited using 200 ms depolarizing steps (-60 mV to 50 mV) from a holding potential of -80 mV, in 10 mV increments. The currents were normalized to cell capacitance. The resulting I-V relationships are shown for cells overexpressing GFP, BID or C-BID before (**A,** Total current) and after (**B,** nifedipine- resistant current) exposure of cells to 10 μM nifedipine. **C,** The I-V relationship for nifedipine-sensitive Ca^{2+} current was obtained by subtracting the nifedipine-resistant current from total current. All I-V relationships (**A, B, C**) were significantly suppressed by overexpression of BID and C-BID compared to the control construct, GFP (n = 4-5 each point).

Figure 8. **A,** Western blot confirming that HL-1 cells express L-type ($Ca_V1.2$ and $Ca_V1.3$) and T-type ($Ca_V3.1$ and $Ca_V3.2$) Ca^{2+} channels. The molecular weights for the proteins of interest were: $Ca_V1.2$, 190-240 kDa; $Ca_V1.3$, 250 kDa; $Ca_V3.1$, 240 kDa; and $Ca_V3.2$, 230 kDa). **B,** Low threshold current was elicited by progressive 10-mV pulses from -80 mV to -10 mV in Control solution in HL-1 cells overexpressing GFP, C-BID and BID (top traces). The transient current was reduced by 7 μM mibefradil, a preferential blocker of T-type channels (lower traces). **C,** The bar diagram shows the peak mibefradil-sensitive Ca^{2+} current density at -10 mV, which was calculated as the difference between the peak Ca^{2+} current density at -10 mV before and after the treatment with mibefradil. There was no significant difference in mibefradil-sensitive Ca^{2+} current between the 3 groups of cells (n= 4-5).

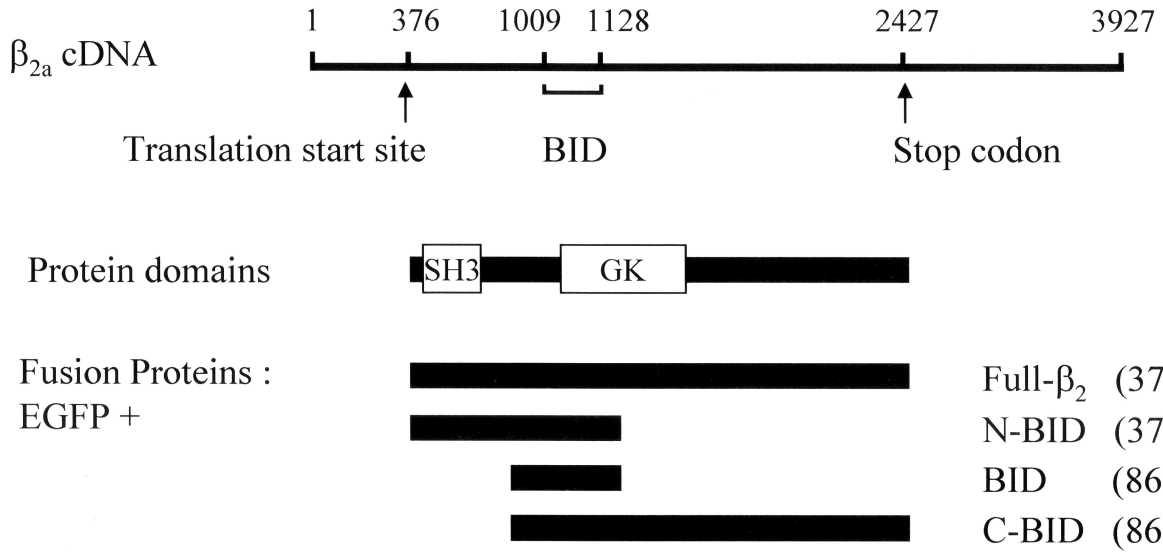

Figure 1

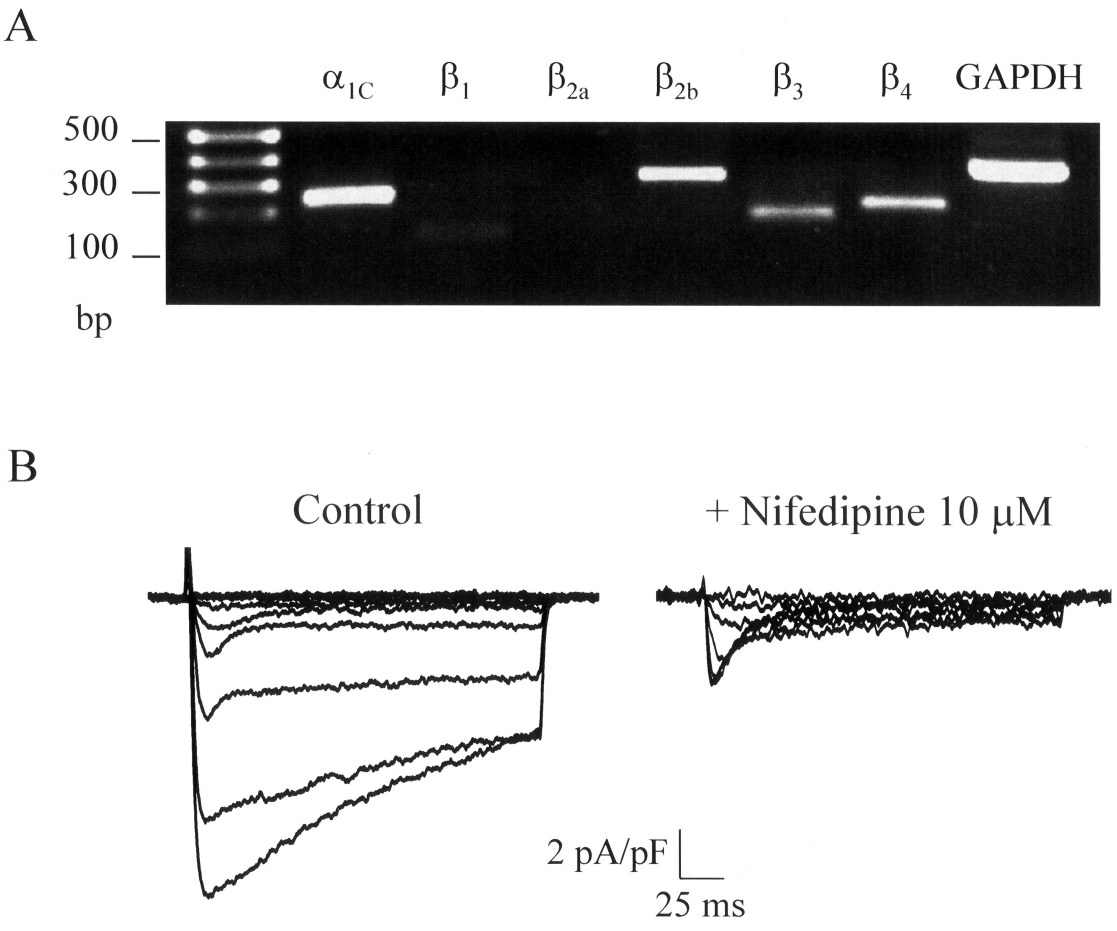

Figure 2

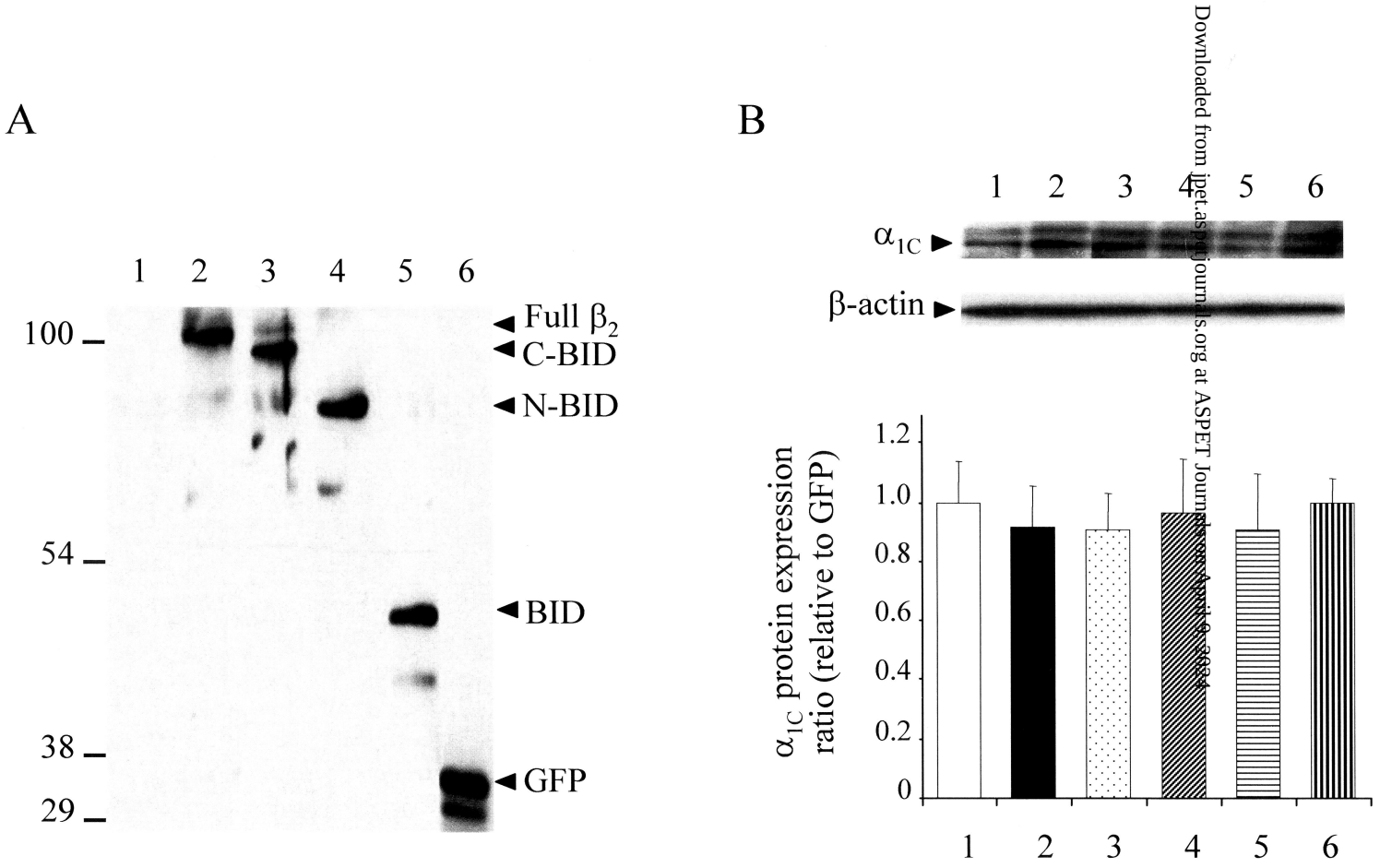

Figure 3

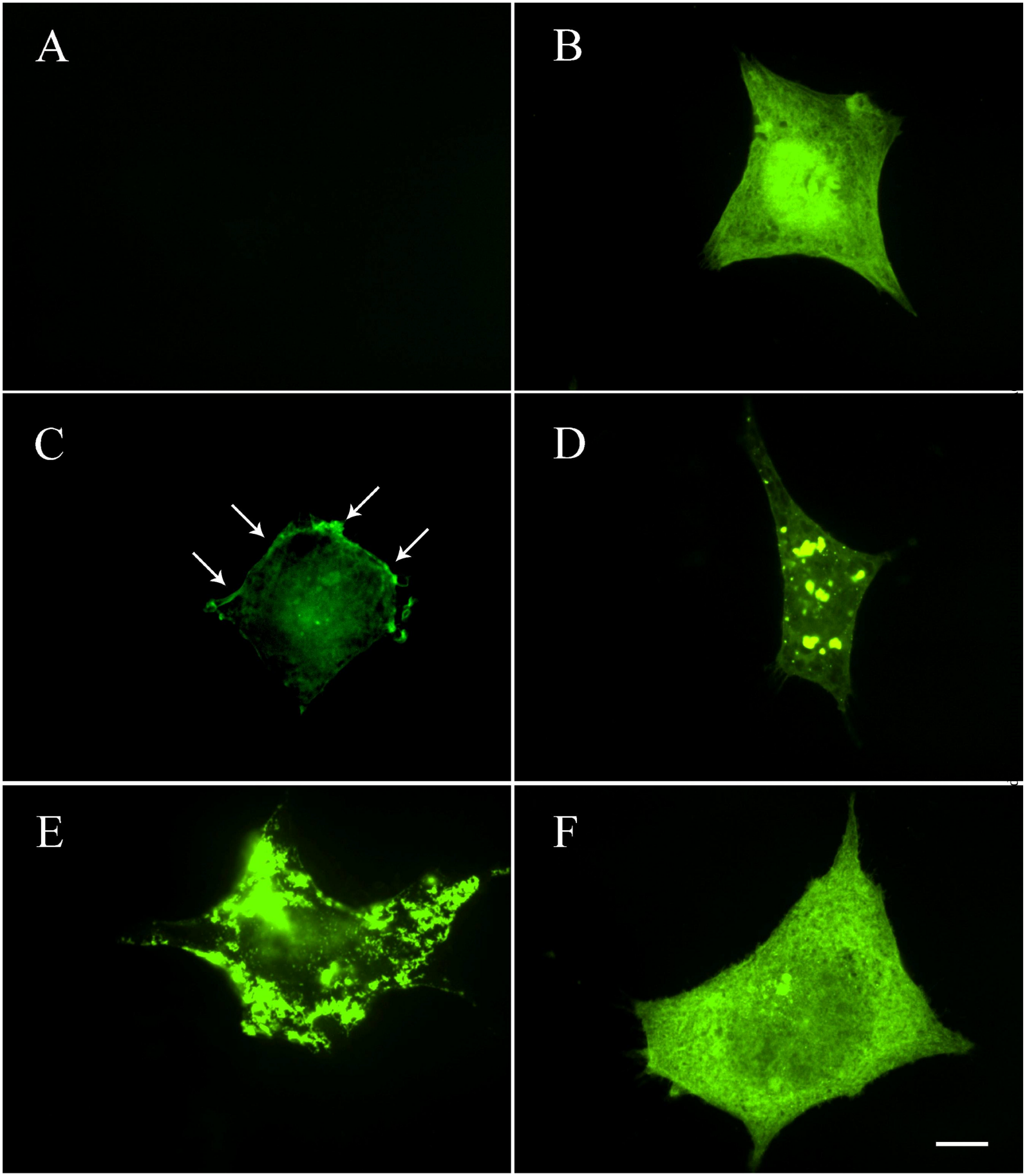

Figure 4

JPET Fast Forward. Published on January 9, 2008 as DOI: 10.1124/jpet.107.128215
This article has not been copyedited and formatted. The final version may differ from this version.

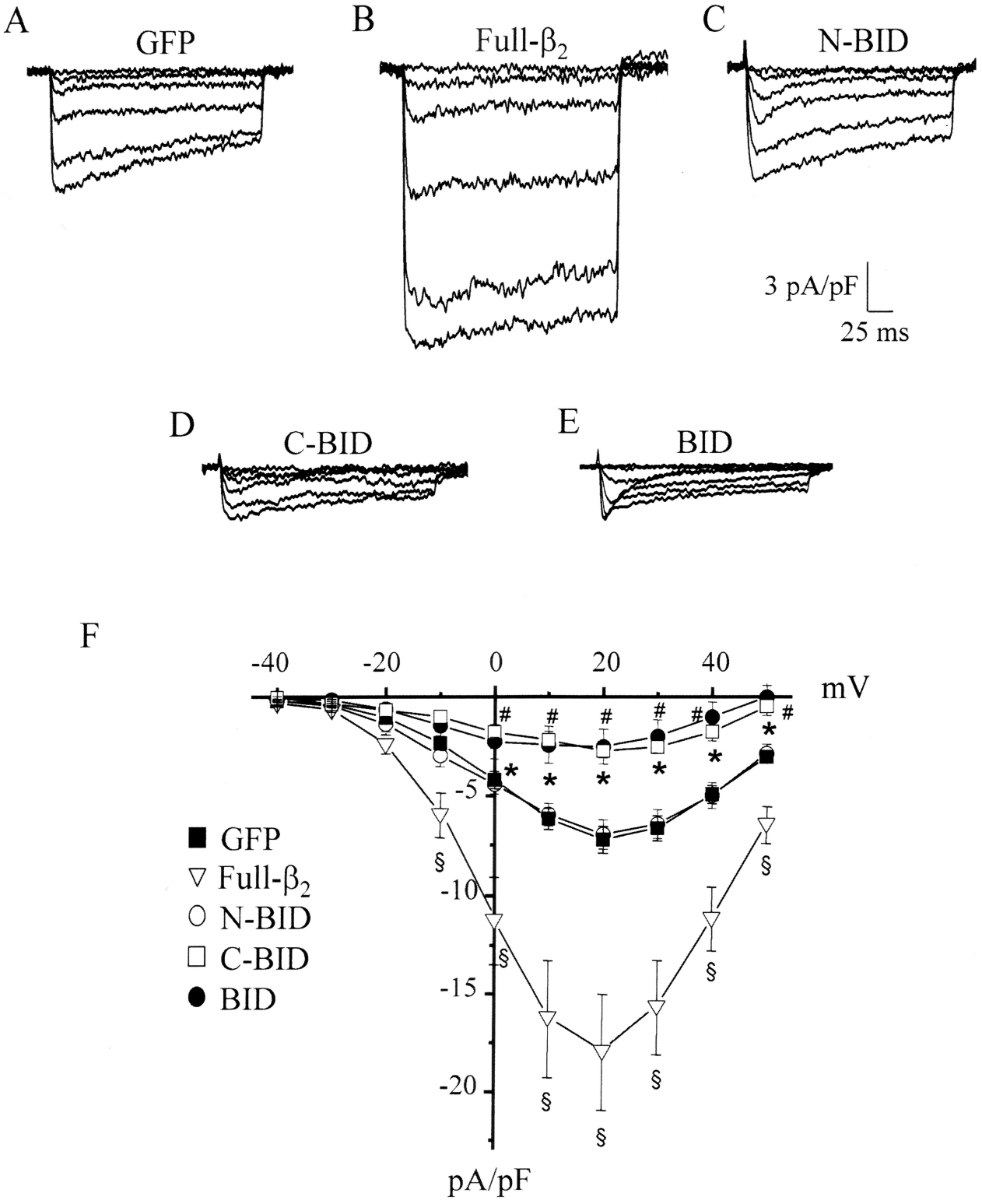

Figure 5

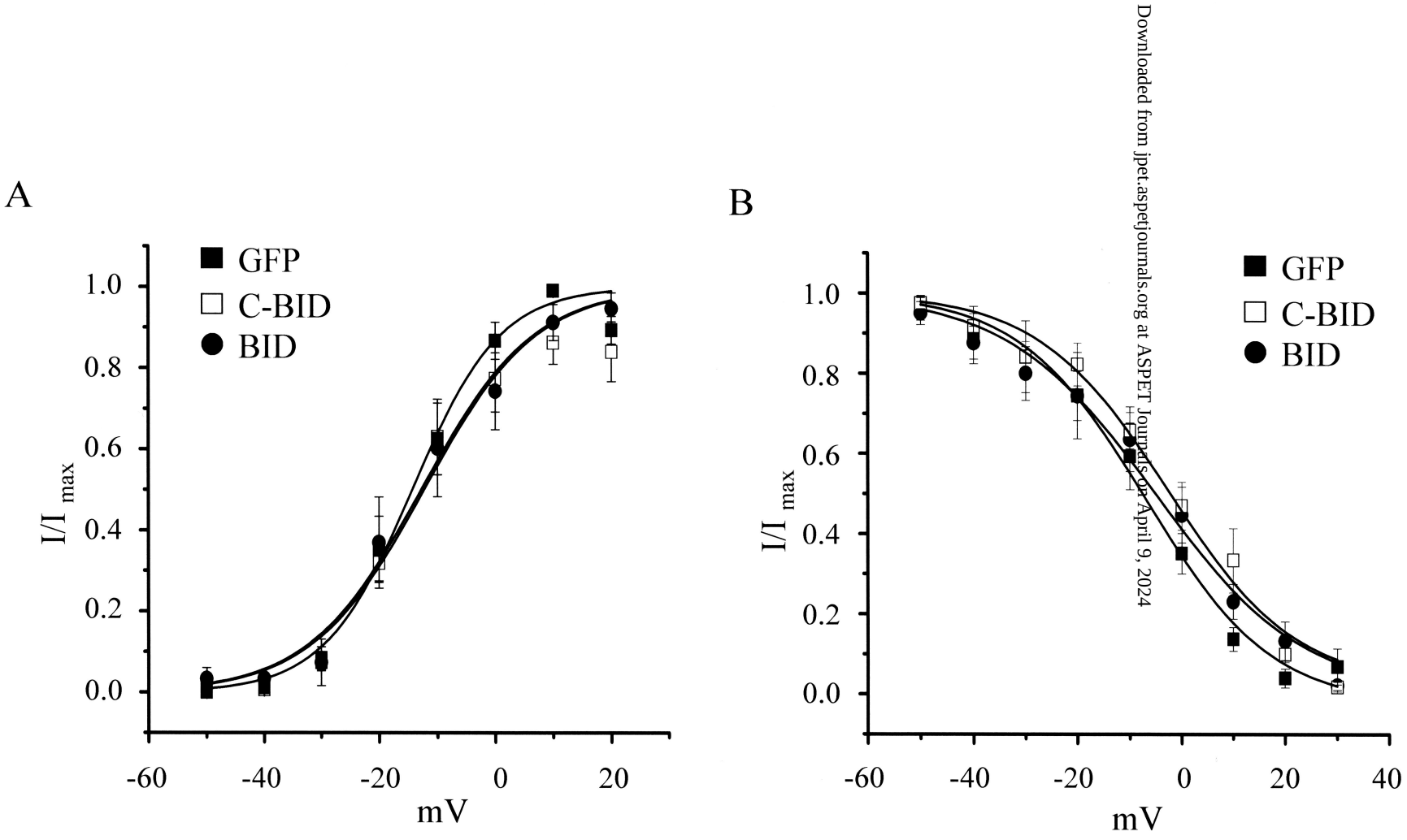

Figure 6

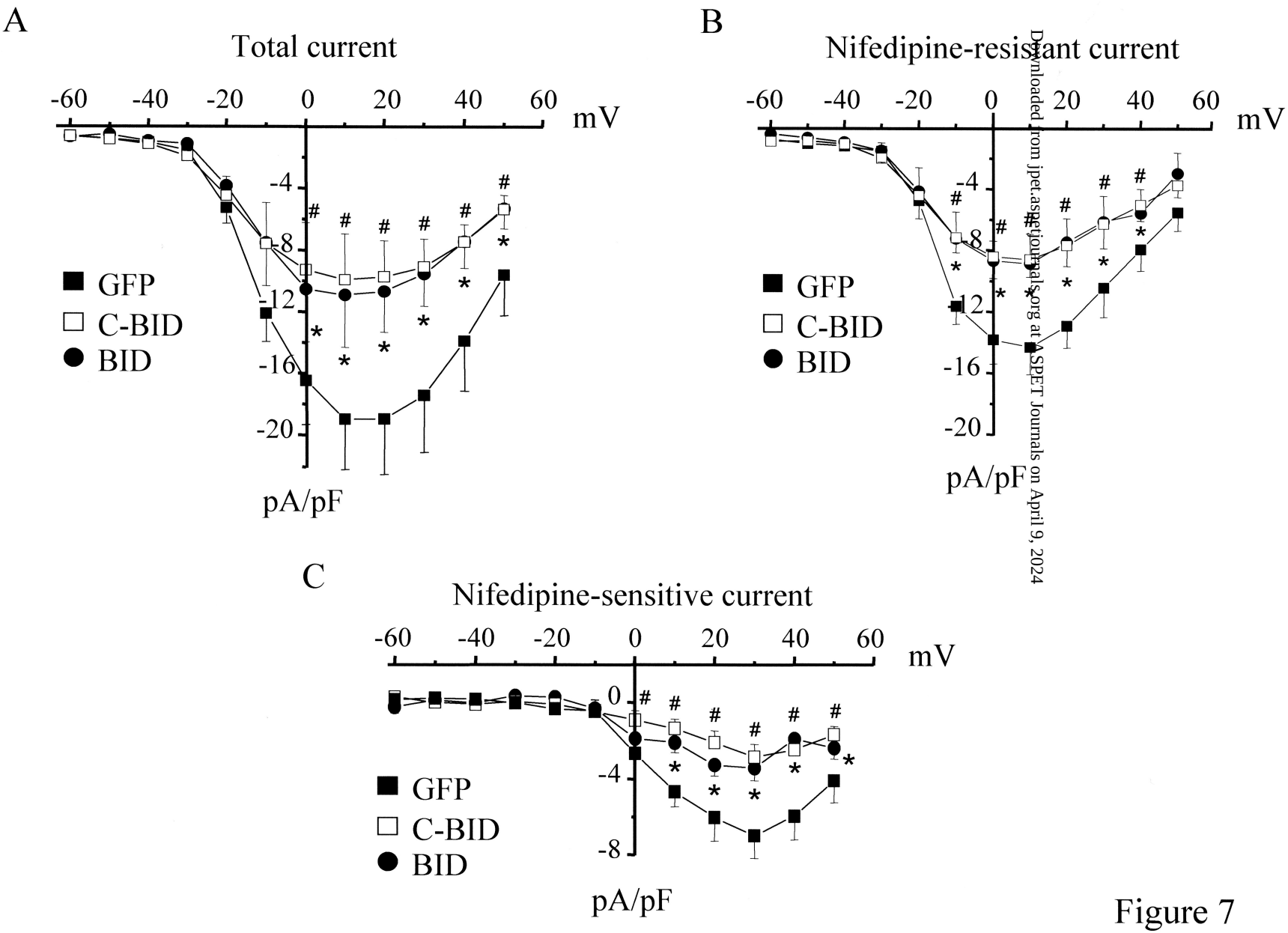

Figure 7

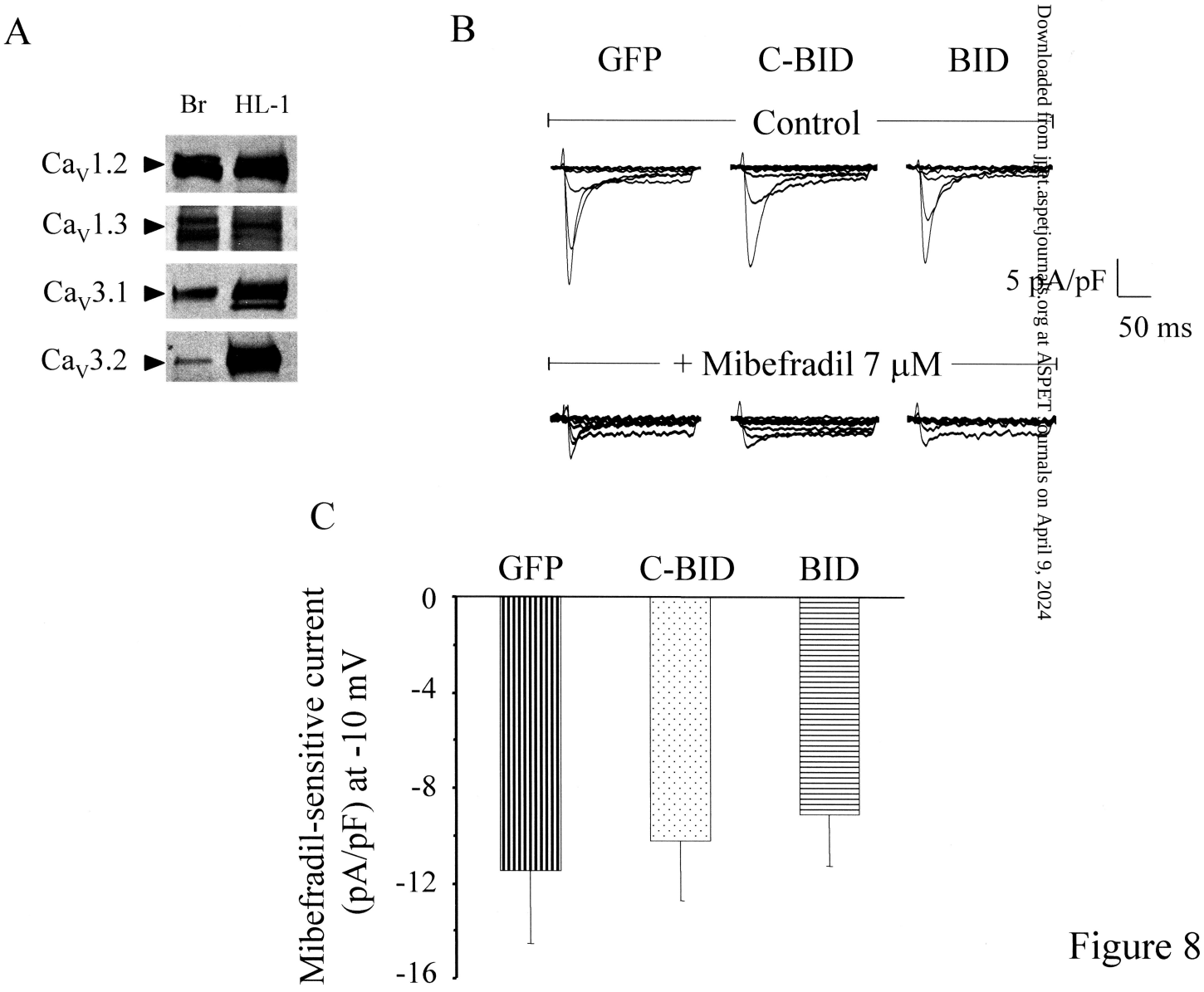

Figure 8